Tungsten-182 in the upper continental crust: Evidence from glacial diamictites

A. Mundl[a,*], R.J. Walker[a], J.R. Reimink[b], R.L. Rudnick[c], R.M. Gaschnig[d]

[a] Department of Geology, University of Maryland, College Park, MD 20740, USA
[b] Department of Terrestrial Magnetism, Carnegie Institute of Washington, Washington, DC 20015, USA
[c] Department of Earth Science and Earth Research Institute, University of California, Santa Barbara, CA 73106, USA
[d] Department of Environmental, Earth and Atmospheric Sciences, University of Massachusetts Lowell, Lowell, MA 01854, USA

ARTICLE INFO

ABSTRACT

Study of igneous and sedimentary rocks that may be representative of the chemical and isotopic characteristics of portions of the upper continental crust (UCC) has provided important insights to the origin and growth of the continents, as well as the large-scale chemical evolution of the silicate Earth. For example, changes in the major and trace element compositions, as well as long-lived radiogenic isotope systematics of (meta)sedimentary rocks through time have led to the conclusion that at least some portions of the Archean UCC were enriched in mafic-ultramafic components compared to UCC with younger provenance (Taylor and McLennan, 1985; Condie, 1993; Gaschnig et al., 2016; Chen et al., 2016; Tang et al., 2016; Garçon et al., 2017). Short-lived radiogenic isotope systems are an additional means of tracing the contributions of diverse mantle-derived components to the UCC. Tungsten-182 anomalies have been observed in both ancient and modern rocks. Although these anomalies were ultimately created by processes that occurred while ^{182}Hf was extant during the first ~60 Ma of Solar System history, the causes of their incorporation and preservation in the rock record, as well as the frequency and distribution of rocks in the UCC with isotopic anomalies remain poorly understood. Here, μ^{182}W values (deviations in ^{182}W/^{184}W from laboratory reference standard in parts per million) are reported for previously well-characterized, fine-grained glacial diamictites deposited between ~3.0 and ~0.3 Ga. Glacial diamictites deposited during the Mesoarchean as part of the Witwatersrand Supergroup in southern Africa are characterized by an average μ^{182}W value of -12.5 ± 5.0 (2SD), yet a diamictite of similar age from the spatially associated Pongola Supergroup (Mozaan) is not isotopically anomalous. The isotopically anomalous diamictites are also characterized by comparatively high Ni and highly siderophile element (HSE) abundances, indicative of significant contributions from ultramafic, most likely komatiitic components. No resolvable ^{182}W anomalies were found in glacial diamictites with lower Ni and HSE, deposited after 2.3 Ga. This in turn suggests that W isotopic anomalies in Archean UCC, at least in part, reflect contributions from deep mantle upwellings that produced some of the komatiites. The new results provide further evidence that the isotopic composition of W in the Archean crust was highly variable.

1. Introduction

The upper continental crust (UCC) can be viewed as the geochemical distillate of materials originating in the upper mantle. Consistent with this, the UCC is strongly enriched in incompatible elements relative to the bulk silicate Earth (BSE) (Rudnick and Gao, 2014). Chemical and isotopic changes in the composition of rocks believed to be representative of the UCC through time, therefore, likely reflect changes in the nature of the building blocks of the continental crust, as well as the mantle sources from which the building blocks were

ultimately derived (e.g., Dhuime et al., 2012). Materials that have been interrogated in order to track changes in the chemical composition of the UCC through time include sedimentary rocks such as shales and metamorphosed equivalents, and granites formed through the melting of metasedimentary precursors (e.g., Shaw et al., 1976; Taylor and McLennan, 1985; Condie, 1993; Gao et al., 1998).

Another type of sedimentary rock that has been examined to explore the chemical evolution of the UCC is glacial diamictite. Throughout its history, Earth has undergone extreme climatic changes that resulted in periods of widespread glaciation and resulting mechanical surface
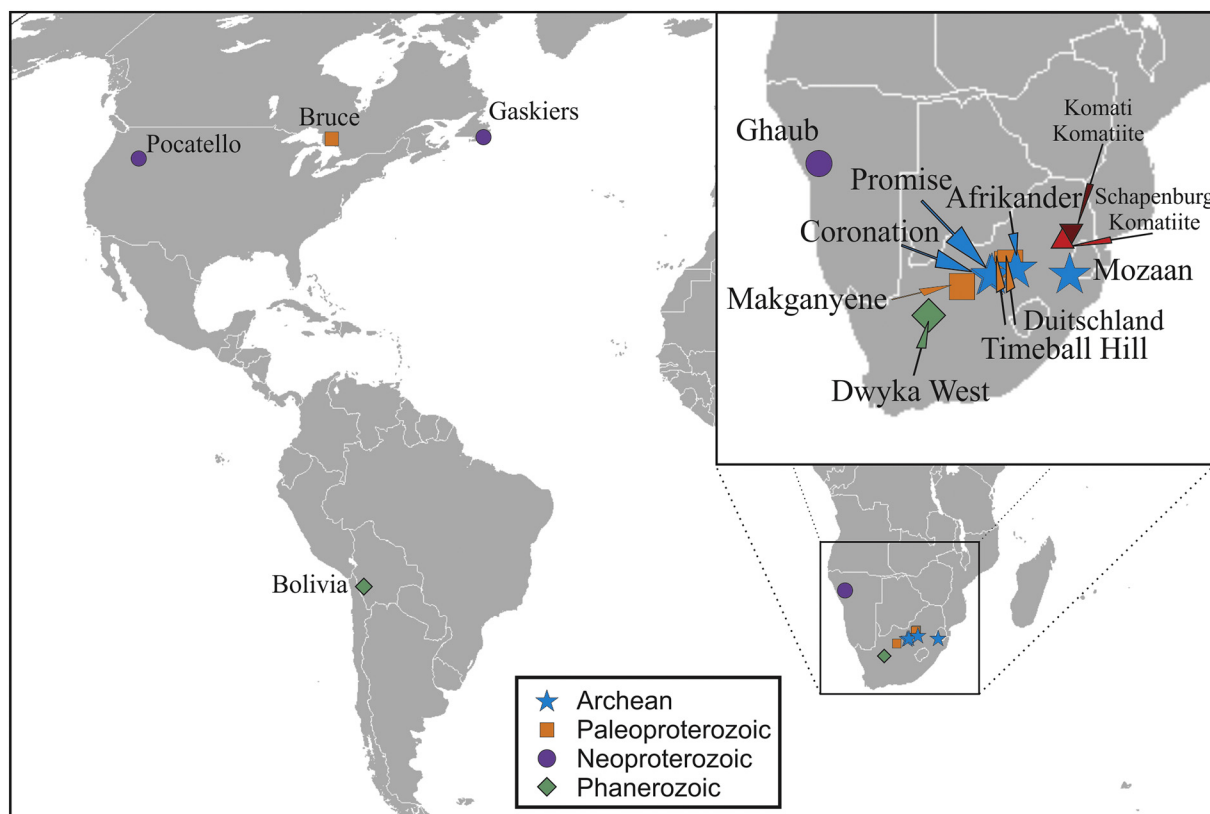
Fig. 1. Global map showing the diamictite composite sample localities. Different symbols represent the eons during which glacial diamictites were deposited as presented in Gaschnig et al. (2016). Triangle and upside down triangle show the location of the Schapenburg and Komati komatiites, respectively.

erosion. The episodes of glaciation led to production and deposition of sediments that provide a representative sampling of the glaciated UCC. Once lithified, the resulting glacial diamictite may record both chemical and isotopic compositions of a limited portion of the UCC with high fidelity, due to the limited chemical alteration imparted by the low temperature, largely mechanical glaciation processes. Although the sampling of only localized provenance limits the global applicability of individual glacial diamictites, similarities in some geochemical trends for diamictites of the same age from different localities suggests that their geochemical characteristics may reflect global trends in the composition of the UCC. For example, major and trace element variations in glacial diamictites through time suggest that average Archean UCC had a larger proportion of mafic, and especially ultramafic (komatiitic) inputs, compared to glacial diamictites with younger provenance (Gaschnig et al., 2014, 2016). This difference is particularly apparent in the higher concentrations of Ni and highly siderophile elements (HSE: e.g., Re, Os, Ir, Ru, Pt, Pd) in diamictites from older provenances compared with younger (Chen et al., 2016).

Trace element and long-lived radiogenic isotope systems in shales and other terrigenous sedimentary rocks can also be used to characterize the changing composition of the UCC. For example, Taylor and McLennan (1985) showed a step-wise increase in Th/Sc in shales at the Archean-Proterozoic boundary that was attributed to a decrease in mafic source components in the younger sediments. Later, Condie (1993) used both surface samples and shales to suggest that the Archean UCC contained a greater abundance of basalt and komatiite compared to post-Archean UCC. More recently, Tang et al. (2016), using Ni/Co and Cr/Zn ratios in sedimentary rocks, suggested that the MgO content of the UCC dropped from a high of ~15% at 3.2 Ga to values near present-day estimates for UCC of ~4% at the Archean-Proterozoic boundary. Further, Garçon et al. (2017) examined the $^{143}Nd/^{144}Nd$ and $^{176}Hf/^{177}Hf$ isotopic compositions of Archean metasedimentary rocks from the Barberton area, southern Africa. Consistent

with the conclusions of Gaschnig et al. (2016) and Chen et al. (2016), that study also concluded that the Archean UCC sampled by the metasedimentary rocks was more mafic than modern UCC.

Short-lived radiogenic isotope systems, such as ^{182}Hf-^{182}W may also provide important insights into the origin and evolution of the UCC. Anomalies in both ancient and modern terrestrial rocks have been observed for this system ($^{182}Hf \rightarrow ^{182}W + 2\beta^-$; $T_{1/2} = 8.9$ Ma; Vockenhuber et al., 2004). Isotopic anomalies appear to have been common in Paleoarchean supracrustal rocks (e.g., Willbold et al., 2011; Touboul et al., 2014; Liu et al., 2016; Reimink et al., 2018), as well as in komatiites as young as 2.7 Ga (e.g., Touboul et al., 2012; Puchtel et al., 2016). Reported $\mu^{182}W$ values (deviations in $^{182}W/^{184}W$ from laboratory reference standard in parts per million) for early Archean supracrustal rocks have nearly all been positive, while values for komatiites range from positive to negative. With the exception of some volumetrically small young ocean island basalts (Mundl et al., 2017) and flood basalts (Rizo et al., 2016a) that likely derived from deep-seated mantle sources, the limited existing data suggest that post-Archean rocks are largely devoid of ^{182}W anomalies. This may indicate that the upper mantle has been homogeneous with respect to W isotopes after the Archean, with subsequent contributions to the continental crust from the upper mantle reflecting this.

Here, we report ^{182}W isotopic data for glacial diamictites that were deposited during the Archean through the Phanerozoic. We analyzed a subset of composite samples studied for major and trace elements including HSE, as well as oxygen, lithium and barium stable isotopes by Gaschnig et al. (2016), Li et al. (2016), Chen et al. (2016) and Nan et al. (2018). The primary objective is to assess whether or not W isotopic anomalies are present in these rocks, and if so, whether the anomalies can be correlated with other chemical or isotopic characteristics. In order to evaluate the average age of the diamictite provenance, we also analyzed six of the same rocks for their ^{147}Sm-^{143}Nd isotopic systematics.

2. Samples

Thirteen diamictite composites were analyzed for W concentration and isotopic composition. Each composite was constructed from equal parts by weight of multiple samples from within the same diamictite unit. Thorough mixing of the composite materials is assumed to have resulted in the production of homogeneous sample powders. The diamictite composites can, therefore, be considered representative of the glacially sampled UCC at each location at the time of deposition. Additional details regarding the preparation of the diamictite composites, major and trace element compositions, as well as highly siderophile element (HSE) abundances and Li, O, Ba and Re-Os isotopic compositions of individual diamictites, as well as the composites were previously reported (Gaschnig et al., 2014, 2016; Li et al., 2016; Chen et al., 2016; Nan et al., 2018).

The diamictites were deposited during the Mesoarchean to Paleozoic. They sample three different continents, North and South America and Africa (Fig. 1). All of the Archean diamictites are from South Africa, and three of those glacial deposits occur in the Witwatersrand Supergroup (Promise, Afrikander, and Coronation). An additional Archean diamictite was collected from the Pongola Supergroup (Mozaan), located to the southeast of the Witwatersrand Supergroup. Paleoproterozoic glacial diamictites were sampled within the Transvaal Supergroup in South Africa (Makganyene within the Griqualand West Basin; Timeball Hill and Duitschland in the Eastern Transvaal Basin) and the Huronian Supergroup in North America (Bruce). Neoproterozoic diamictites were sampled in the Otavi Group in Namibia (Ghaub) and in two localities in North America (Pocatello and Gaskiers). The youngest diamictites are from the Paleozoic Dwyka Group (Dwyka West, South Africa) and the diamictites of the Machareti and Mandiyuti groups from Bolivia, South America.

In addition to the diamictite samples, we re-analyzed three Schapenburg komatiite samples from the Barberton Greenstone, South Africa, that were previously studied by Puchtel et al. (2016), as these komatiites may be typical of possible precursor rocks to the Archean glacial diamictites from southern Africa. The Puchtel et al. study used [183]W as part of a second order correction for mass spectrometric fractionation (Touboul and Walker, 2012). It has recently been suggested that [183]W might be preferentially retained through laboratory chemical processing of samples, which if true, could lead to systematic errors in earlier measurements that utilized this protocol (Kruijer and Kleine, 2018). Although subsequent studies from our lab that utilized a different method to independently measure [183]W show no selective loss of that isotope in the chemical processing of samples (Archer et al., 2017; Mundl et al., 2017), we re-examined several of the Schapenburg suite to confirm the earlier results.

3. Analytical methods

3.1. Tungsten concentrations and isotopic compositions

Tungsten concentrations were determined by isotope dilution. Approximately 100 mg of sample were digested together with a [182]W spike in ~6 ml of 5:1 HF:HNO₃ for 3 days at ~150 °C. After complete dissolution, samples were dried down and converted into chloride form by adding 2 ml 6 M HCl and subsequently evaporated to dryness. Residues were then re-dissolved in 0.5 M HCl- 0.5 M HF and W was separated using a previously established anion column chemistry procedure similar to that described in Kleine et al. (2004). Tungsten concentrations were measured using a *Nu Plasma* multi-collector ICP-MS at the University of Maryland.

For the determination of W isotopic compositions, between 0.5 and 7 g of sample powder were digested in Teflon vials using 20–50 ml of a concentrated mixture of HF and HNO₃ (5:1) for 5 days at ~150 °C. After evaporation to dryness, samples were treated with HNO₃ and several drops of H₂O₂ to remove organics. The dried down residues were then converted into chloride form by adding ~5 ml of 8 M HCl. After subsequent evaporation to dryness, samples were re-dissolved in 20–70 ml of 1 M HCl-0.1 M HF, centrifuged and the supernatant was used to separate W in a four-step ion exchange chromatography method, slightly modified from that of Touboul and Walker (2012). The most significant modification of the column chemistry protocol from Touboul and Walker (2012) is the replacement of 6 M HAc-8 mM HNO₃-1%H₂O₂ with 0.09 M HCt-0.4 M HNO₃-1%H₂O₂ to elute Ti. Total W recovery was between 65 and 90% for all samples. The analytical blank is composed of a digestion blank, as well as individual column step blanks (4 steps - 1 column blank each) that were measured by isotope dilution on the *Nu Plasma* MC-ICP-MS and summed according to the number of columns used per step per sample. The W blank for the sample with the largest number of columns in Steps 1 and 2 (Afrikander), and thus, the highest blank, resulted in a total of < 1.5 ng W, which corresponds to < 0.3% of the total W in the sample, resulting in negligible blank corrections.

Isotopic compositions were measured by thermal ionization mass spectrometry in negative ionization mode (N-TIMS) using a *Thermo-Fisher Triton* at the University of Maryland. All samples were analyzed using the method described in Archer et al. (2017). The laboratory standard solutions analyzed during the course of this study included an *Alfa Aesar* standard used in the *Isotope Geochemistry Laboratory* at the University of Maryland, as well as an *Alfa Aesar* standard solution obtained from the University of Münster for comparison. Analyses of both standard batches resulted in virtually identical W isotopic compositions (Table S1). We also analyzed *NIST* steel standard *129c*, determining $^{182}W/^{186}W_{N6/4}$, $^{182}W/^{186}W_{N6/3}$ and $^{183}W/^{186}W_{N6/4}$ ratios that are indistinguishable from the *Alfa Aesar* standard solutions (Table S2), and comparable to the value reported by Kruijer and Kleine (2018).

3.2. Sm-Nd concentration and isotopic compositions

Samples were dissolved by flux fusion by adding 70–300 mg of sample powder to ~1 g of a mixture of 67% lithium tetraborate - 33% lithium metaborate and ~0.01–0.05 g lithium bromide. This mixture was heated for ~15 min in graphite crucibles at 1050 °C in a muffle furnace. The sample was removed from the furnace, swirled to promote homogenization, and then quenched in 2 N HNO₃ and filtered. After dissolution by flux fusion, ~10% of the sample aliquot was spiked with a mixed $^{149}Sm-^{150}Nd$ tracer. Samarium and Nd of the spiked aliquot were separated using *LN Spec* cation resin and Sm and Nd were measured using a *Triton* TIMS instrument at the Department of Terrestrial Magnetism using a double filament arrangement and a static collection routine. Neodymium isotopic compositions for these spiked samples were fractionation corrected to $^{146}Nd/^{144}Nd = 0.7219$ using the exponential law while Sm was fractionation corrected to $^{147}Sm/^{152}Sm = 0.56081$ using the exponential law.

4. Results

4.1. Tungsten concentrations and ^{182}W isotopic compositions

The strongly incompatible behavior of W during mantle melting has resulted in an overall enrichment of W in the continental crust, relative to primitive mantle estimates (Arevalo Jr. and McDonough, 2008). Bulk rock W concentrations of the diamictite composites range from 600 to 4100 ppb and broadly correlate with similarly incompatible trace elements, such as Th (Fig. 2). Overall, incompatible lithophile trace element compositions, as well the siderophile W, are lower in the Archean diamictites compared to Proterozoic and Phanerozoic samples (Gaschnig et al., 2016). For example, the Archean diamictites have W concentrations ranging from 600 to 720 ppb whereas samples deposited later have concentrations ranging from 930 to 4100 ppb (Table 1).

Tungsten isotopic compositions are reported in Tables 1 and 2 and shown in Figs. 3 and 4. All samples have been analyzed multiple times,
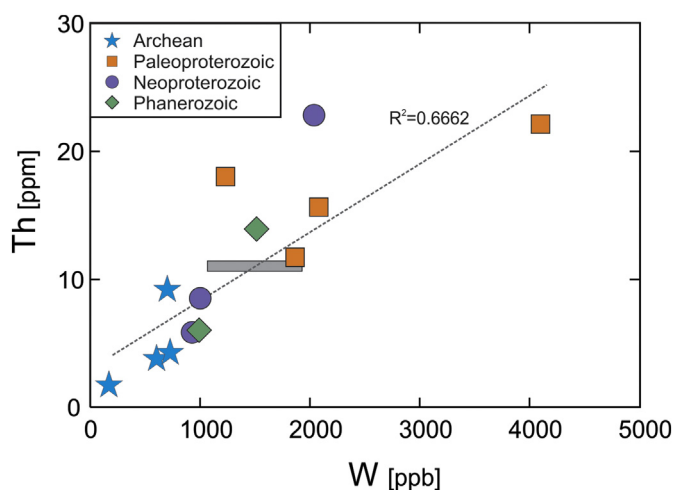
Fig. 2. Th in parts per million (ppm) vs. W in parts per billion (ppb) showing a good positive correlation. Light grey striped box represents the average composition of UCC (Th = 10.5–11.3 ppm; W = 1.1–1.9 ppm), from Rudnick and Gao (2014) and Gaschnig et al. (2016). Legend as in Fig. 1.

as separate digestions (indicated in Table 1 as duplicate); from the same digestion and chemical separation, but loaded and analyzed on different filaments during separate analytical sessions; or the samples on filaments have been re-activated by addition of more of the La-Gd electron emitter solution, following an initial analysis, then re-analyzed.

Most of the Archean diamictites from South Africa are characterized by negative ^{182}W anomalies. Samples from the Witwatersrand group (Promise, Coronation, and Afrikander) yield μ^{182}W values down to -14 ± 4.5 ppm. By contrast, the μ^{182}W value of -4.2 ± 4.5 for the Mozaan diamictite is not resolved from the 2SD or the 2SE of the standard. The Paleoproterozoic Makganyene diamictite shows a small negative μ^{182}W value of -6.4 ± 4.5 that is just resolved from the 2SE of the laboratory standard (0 ± 1.5), but not from the 2SD of the standard (0 ± 4.5). None of the other samples deposited during the Paleoproterozoic, Neoproterozoic or Paleozoic are characterized by resolved deviations from the 2SE of the standard.

The three Schapenburg komatiites analyzed here are characterized by an average μ^{182}W value of -8.7 ± 4.5 (2SD; Table 2), which is in very good agreement with the average μ^{182}W value of -8.4 ± 4.1 (2SD, n = 10) reported by Puchtel et al. (2016).

4.2. Sm-Nd isotope systematics

Six of the 13 diamictite composites were analyzed for ^{143}Nd/^{144}Nd and ^{147}Sm/^{144}Nd (Table 3, Fig. 5). All six samples are southern African diamictites, two samples each were deposited during the Archean (Promise, Coronation), the Paleoproterozoic (Makganyene, Timeball Hill), one sample was deposited during the Neoproterozoic (Ghaub), and one during the Phanerozoic (Dwyka West). Deposition ages of the diamictites (Table 1) generally reflect either maximum or minimum ages that were determined by U-Pb zircon dating of the immediately under- or overlying stratigraphic units. The Sm-Nd T_{DM} model ages for the diamictites are in all cases older than their ages of deposition.

While the Archean Promise and Coronation diamictites yield slightly older T_{DM} ages than their estimated deposition ages, the samples deposited during the Paleoproterozoic (Makganyene and Timeball Hill) yield Archean model ages (Fig. 5, Table 3). The Ghaub diamictite, deposited during the Neoproterozoic Marinoan glaciation, is characterized by a Paleoproterozoic model age. The largest age difference was determined for the Dwyka West sample. It was deposited during the Phanerozoic (~0.3 Ga) but yields a much older, Archean T_{DM} age, indicating large contributions from Archean crust.

5. Discussion

One key question in any study of ancient rocks is whether or not the chemical/isotopic compositions of the rocks reflect their original characteristics. Tungsten is a fluid mobile element that is enriched in the UCC, so there is a danger of isotopic resetting. The observed correlation of W with Th, an equally incompatible but non-fluid mobile element (e.g., Langmuir and Herman, 1980), however, suggests that the W abundances, and by inference the isotopic compositions, have not been altered by fluid-related surface processes (Fig. 2). Thus, the W concentrations and ^{182}W isotopic compositions of these glacial diamictites most likely reflect the characteristics inherited from their provenance.

The chemical and isotopic characteristics of glacial diamictites have been used in prior studies to track changes in the nature of the UCC through time. For example, major and trace element studies of glacial diamictites record a change in the UCC from more mafic-ultramafic to more felsic compositions, proceeding from the Archean to the Proterozoic and Phanerozoic (e.g., Gaschnig et al., 2016). This compositional change may reflect the onset of plate tectonics and the consequent subduction, recycling and re-melting of basaltic crust to give rise to more evolved continental crust (Dhuime et al., 2015; Tang et al., 2016). Additionally, a reduced heat flux, a consequence of on-going cooling of Earth's interior over billions of years, may have resulted in a decrease in melt production reflected in the generation of significantly lower amounts of komatiitic crust since the Archean (Herzberg et al., 2010). A reduction in the komatiitic component to the UCC since the Archean is indicated by the higher concentrations of Ni and some HSE (Os, Ir and Ru) in Archean diamictites compared to younger diamictites (Chen et al., 2016). This is a reflection of the fact that komatiites tend to have much higher concentrations of these elements than felsic or mafic rocks.

All three diamictites associated with the Mesoarchean Witwatersrand group have well-resolved negative anomalies, with μ^{182}W values averaging ~ -12.5 ± 5.0 (2SD, n = 8). By contrast, the μ^{182}W value of the Mesoarchean Mozaan diamictite, associated with the Pongola Supergroup, is not resolved from the standard value. These observations, coupled with the mostly positive μ^{182}W values for Paleoarchean supracrustal rocks (Willbold et al., 2011; Touboul et al., 2014; Rizo et al., 2016b; Liu et al., 2016; Dale et al., 2017; Reimink et al., 2018), and μ^{182}W values ranging from negative, through normal, to positive for Archean komatiites (Touboul et al., 2012; Puchtel et al., 2016; Puchtel et al., 2018), strengthens the case that the W isotopic composition of the Archean crust was quite variable.

The magnitude of the negative anomalies for the diamictites associated with the Witwatersrand Supergroup is noteworthy in that the anomalies are more negative than any Archean rock previously analyzed. In fact, the only other Archean rocks currently known to have negative μ^{182}W values are the 3.55 Ga Schapenburg komatiites (Puchtel et al., 2016). Given their current spatial association with the Witwatersrand Supergroup diamictites (Fig. 1), they are potential candidates for contributing material with negative μ^{182}W values to these diamictites. The average μ^{182}W value of the Schapenburg komatiites reported by Puchtel et al. (2016) is -8.4 ± 4.1, and our new data for three of these is essentially identical (Fig. 4). The average of all Schapenburg analyses, including the data obtained in this study, is μ^{182}W of -8.5 ± 1.1 (2SE, n = 15), which is distinctly less negative than repeated analysis of the Witwatersrand Promise diamictite sample with μ^{182}W = -13.6 ± 2.5 (2SD, n = 3, Fig. 4). This indicates that crustal rocks with more negative μ^{182}W than recorded in the Schapenburg komatiites, and likely more negative than the diamictite composite averages from this area, were at or near the surface at the time of diamictite deposition. Negative μ^{182}W values of ≤ -14 are present in some modern ocean island basalts (Mundl et al., 2017), so the existence of igneous rocks bearing a similar or more negative μ^{182}W composition during the Archean is plausible, but not yet confirmed by

Table 1

Tungsten concentrations and isotopic compositions. Deposition ages are taken from Gaschnig et al. (2016). $\mu^{182}W$ values (the deviation of $^{182}W/^{184}W$ of a sample from that of a standard in parts per million) are reported as normalized to both $^{186}W/^{183}W$ and to $^{186}W/^{184}W$, respectively. $\mu^{183}W$ is normalized to $^{186}W/^{184}W$. *Error given is the $2\times$ standard error (2SE) of the individual analysis. The error on the average is the $2\times$ standard deviation (2SD) of the standards representing the long-term reproducibility of W measurements. W concentrations are in parts per billion (ppb). dup – duplicate analysis including separate digestion and chemical W separation; reac – re-run of a re-activated filament during a different analytical session. To re-activate a sample, 1 μl of activator solution containing 5 μg each of La and Gd was added to an already run filament; sep. filament – sample from the same digestion and W chemical separation was split onto two separate Re filaments and analyzed during different analytical sessions. Minimum to maximum glacial deposition ages from [1]Mukasa et al. (2013), [2]Kositcin and Krapež (2004), [3]Rasmussen et al. (2013), [4]Keeley et al. (2013), [5]Bowring et al. (2003), [6]Prave et al. (2016), [7]Starck and del Papa (2006), [8]Isbell et al. (2008).

Deposition Eon	Age [Ma]	Sample	$\mu^{182}W_{[N6/3]}$	2SE or 2SD*	$\mu^{182}W_{[N6/4]}$	2SE or 2SD*	$\mu^{183}W_{[N6/4]}$	2SE or 2SD*	W [ppb]
Archean	2935–2981[1]	**Promise**	−14.7	3.7	−15.1	4.7	0.3	4.0	718
		Dup	−12.3	3.5	−14.8	4.7	−1.3	4.4	
		Reac	−13.8	5.9	−12.6	7.6	0.1	6.9	
		Average	**−13.6**	**4.5***	**−14.2**	**6.1***	**−0.3**	**6.5***	
	2935–2981[2]	**Afrikander**	−10.2	3.0	−10.8	4.0	−0.5	3.5	170
		Reac	−16.6	3.4	−14.5	4.4	3.5	3.9	
		Average	**−13.4**	**4.5***	**−13.2**	**6.1***	**1.5**	**6.5***	
	2935–2981[2]	**Coronation**	−8.9	3.0	−8.6	3.9	2.1	3.4	702
		Dup	−12.1	6.4	−8.2	7.8	4.0	6.7	
		Reac	−10.9	3.3	−6.3	4.3	2.7	3.8	
		Average	**−10.7**	**4.5***	**−7.7**	**6.1***	**2.9**	**6.5***	
	2954–2980[2]	**Mozaan**	−7.8	3.2	−7.1	4.0	−1.0	3.7	604
		Dup	2.4	3.3	2.1	4.3	0.2	3.9	
		Sep. filament	−6.5	3.3	−7.7	4.2	−1.1	3.7	
		Reac	−5.1	3.5	−0.9	4.6	0.5	4.0	
		Average	**−4.2**	**4.5***	**−3.4**	**6.1***	**−0.3**	**6.5***	
Paleoproterozoic	2222–2431[3]	**Makganyene**	−4.1	3.3	−7.6	4.3	−4.0	4.4	1866
		Reac	−8.7	3.6	−5.1	4.5	−1.6	4.1	
		Average	**−6.4**	**4.5***	**−6.3**	**6.1***	**−2.8**	**6.5***	
	2193–2256[3]	**Timeball Hill**	−4.5	3.5	−4.8	4.3	−0.2	4.0	2082
		Dup	−0.3	3.8	0.2	5.1	−1.9	4.4	
		Average	**−2.4**	**4.5***	**−2.3**	**6.1***	**−1.0**	**6.5***	
	2310–2480[3]	**Duitschland**	−0.5	3.7	−0.5	4.7	−0.4	4.0	4095
		Dup	−2.3	3.9	−1.9	3.9	0.8	3.7	
		Average	**−1.4**	**4.5***	**−1.2**	**6.1***	**0.2**	**6.5***	
	2308–2450[3]	**Bruce**	1.7	3.2	2.9	4.5	−2.0	4.0	1231
		Dup	0.6	4.2	2.8	5.4	−3.0	4.4	
		Average	**1.2**	**4.5***	**2.8**	**6.1***	**−2.5**	**6.5***	
Neoproterozoic	667–705[4]	**Pocatello**	0.3	3.0	1.2	4.0	1.7	3.4	2035
		Dup	2.9	3.2	0.7	4.1	−0.1	3.5	
		Reac	0.4	3.2	5.5	4.3	5.0	3.8	
		Average	**1.2**	**4.5***	**2.5**	**6.1***	**2.2**	**6.5***	
	580–581[5]	**Gaskiers**	−6.1	3.5	−8.5	4.6	−3.1	4.0	1002
		Dup	−1.0	3.3	−5.4	4.4	−4.4	3.8	
		Reac	−0.5	3.4	0.8	4.2	−0.3	3.8	
		Average	**−2.5**	**4.5***	**−4.4**	**6.1***	**−2.6**	**6.5***	
	633–637[6]	**Ghaub**	−5.4	3.3	−4.5	4.4	1.2	4.1	928
		Dup	−6.3	3.5	−9.6	4.4	−5.9	3.6	
		Average	**−5.9**	**4.5***	**−7.0**	**6.1***	**−2.3**	**6.5***	
Phanerozoic	288–312[7]	**Dwyka West**	1.1	3.5	−0.9	4.7	−0.5	4.0	992
		Dup	−3.5	3.7	−4.1	5.2	−1.3	4.6	
		Average	**−1.2**	**4.5***	**−2.5**	**6.1***	**−0.9**	**6.5***	
	299–326[8]	**Bolivia**	0.6	3.5	1.3	4.5	2.9	4.5	1513
		Dup	−3.3	3.1	−1.0	4.2	0.0	3.6	
		Average	**−1.3**	**4.5***	**0.2**	**6.1***	**1.4**	**6.5***	

measurements.

Compared to the Witwatersrand Supergroup diamictite composites, the data for the Mozaan diamictite (Pongola Supergroup) reflect different continental crustal source components, in this case having normal or near normal W isotopic compositions. Similar Nd T_{DM} ages for the Mozaan (3.29 Ga) and Promise (3.31 Ga) formations imply a comparable age distribution of crustal source components with different $\mu^{182}W$ values. It is difficult to reconstruct the path of the glaciers giving rise to the two diamictite groups during the Mesoarchean, so the relative positions of the sources of their sediments remains unknown.

The nature of the crustal materials contributing to the W isotopic compositions of the Mesoarchean diamictites remains poorly constrained. The W isotopic composition of the Mozaan diamictite can be produced by combining any number of components with normal isotopic compositions. For example, the 3.48 Ga Komati komatiites from the spatially associated Barberton Greenstone Belt have no W anomalies (Touboul et al., 2012), and similar materials in the crust could have contributed to the diamictite isotopic composition. The normal isotopic composition could also have been produced by mixing materials with positive and negative anomalies in such proportions that they averaged to define a lack of anomaly.

The broad correlation between $\mu^{182}W$ and elements that is most highly concentrated in komatiites, such as the HSE and Ni (Fig. 6a–b), suggests that komatiites with more negative $\mu^{182}W$ values than the Schapenburg komatiites contributed material to the Witwatersrand group diamictites. This, in turn, may suggest that the contributing komatiites sampled a diversity of early-formed mantle domains that were either accessed less frequently during the subsequent growth of the UCC, or that those domains were largely mixed away by mantle convection. The mantle sources of komatiites likely tap deeper mantle source reservoirs (e.g., Herzberg, 1992; Puchtel et al., 2001) than the upper mantle sources commonly envisioned for the creation of

Table 2

Tungsten isotopic compositions of the Schapenburg komatiites analyzed in this study. $\mu^{182}W$ (the deviation of $^{182}W/^{184}W$ of a sample from that of a standard in parts per million) is normalized to $^{186}W/^{183}W$. $\mu^{183}W$ is normalized to $^{186}W/^{184}W$. Error given is the 2× standard error (2SE) of the individual analysis. *The error on the average is the 2× standard deviation (2SD) of the sample analyses (n = 5). sep. filament – sample from the same digestion and W chemical separation was split onto two separate Re filaments and analyzed during different analytical sessions.

Sample	$\mu^{182}W_{[N6/3]}$	2SE or 2SD*	$\mu^{182}W_{[N6/4]}$	2SE or 2SD*	$\mu^{183}W_{[N6/4]}$	2SE or 2SD*
SCH1.19	−4.9	3.5	−7.4	4.6	−1.3	4.1
Sep. filament	−8.0	3.4	−2.9	4.3	7.6	3.7
SCH1.9	−8.0	3.6	−12.7	4.7	−7.1	4.1
SCH2.2	−12.2	3.6	−10.3	4.6	−0.2	3.9
Sep. filament	−10.3	3.5	−10.1	4.6	−0.2	4.1
Average	**−8.7**	**5.5***	**−8.7**	**7.4***	**−0.2**	**10.4***

Fig. 4. Average $\mu^{182}W$ composition of Archean Witwatersrand group diamictites (stars) and the 3.55 Ga old Schapenburg komatiites. Schapenburg komatiites: small symbols represent individual analysis and large symbols their averages. Samples with hexagonal symbol are from this study (average $\mu^{182}W = -8.7 \pm 4.5$; 2SD, n = 5). Triangles represent samples from Puchtel et al. (2016), ($\mu^{182}W = -8.4 \pm 4.1$; 2SD, n = 10). The filled circle is the average of all Schapenburg analysis (n = 15). The average $\mu^{182}W$ of the Schapenburg komatiites is resolvably higher than the average of the Promise formation.

Fig. 3. $\mu^{182}W$ isotope composition of the diamictites, where $\mu^{182}W$ is the deviation of $^{182}W/^{184}W$ of a sample from the average of repeated analysis of standards in ppm. $\mu^{182}W$ shown is $^{182}W/^{184}W$ normalized to $^{186}W/^{183}W$. Samples are plotted from oldest to youngest deposition ages from the bottom of the figure upwards. Small symbols represent individual analysis of samples. Large symbols are the averages of multiple sample analysis. Light grey bar represents the 2× standard deviation (2SD) of repeated analysis of an *Alfa Aeasar* tungsten standard solution showing the long-term reproducibility of standard measurements (2SD = 4.5 ppm). The dark grey bar represents the respective 2 standard error (2SE = 1.5 ppm). Error bars on the individual data points are the 2SE of the individual sample run. Error bars on the averages represent the 2SD of the standards (4.5 ppm).

continental crust (e.g., Cawood et al., 2013; Hawkesworth et al., 2013). The deeper sources may have been characterized by more heterogeneous ^{182}W signatures much longer into Earth's history than upper mantle-derived rocks.

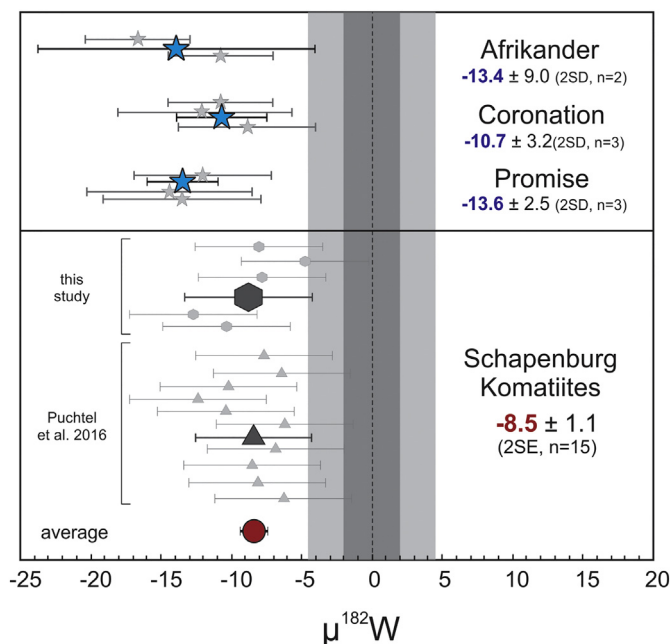Despite the strong chemical evidence for komatiitic contributions to the Mesoarchean diamictites, komatiites cannot be the dominant provenance for at least the major elements in these rocks. Gaschnig et al. (2016) reported bulk SiO_2 for these diamictite composites ranging from 57 wt% (Mozaan) to 72 wt% (Coronation). These are much higher concentrations than are present in typical komatiites (e.g., average of 47 wt% for Schapenburg; Puchtel et al., 2016), so considerable mafic and/or felsic components are required to account for the bulk compositions of these diamictites. The need for additional components to account for the negative W anomalies is not as clear. It remains unknown which phases are the dominant carriers of W in diamictites, so it is possible that the W in the diamictites was acquired from komatiitic sources.

In contrast to the Archean samples, there is more limited W isotopic variability in post-Archean diamictite composites. As noted, the Makganyene composite is characterized by a negative $\mu^{182}W$ value of -6.4 ± 4.5 that is barely resolved from the 2SE of repeated analysis of the laboratory standard solution. Although it has a deposition age of ~2.43 Ga (Rasmussen et al., 2013; Gumsley et al., 2017), its Nd T_{DM} model age is 2.97 Ga, so it likely has an averaged provenance of Archean age. The Timeball Hill diamictite has deposition and T_{DM} ages of 2.26 (Rasmussen et al., 2013) and 2.87 Ga, respectively, that are similar to the ages for Makganyene, but it has no anomaly. Clues to the causes of the difference in the W isotopic compositions for these two diamictites may be found in their detrital zircon age distributions. Zircon U-Pb age distributions for both Makganyene and Timeball Hill formations are broadly similar, with main age peaks at ~2.5 Ga (Moore et al., 2012; Schröder et al., 2016). However, zircon data from the Makganyene diamictite also indicate significant contributions from several much older components, with ages of 3.3, 3.4 and 3.7 Ga (Moore et al., 2012). Detrital zircon data for the Timeball Hill formation, by contrast, show only minor contributions from crust that is older than 2.8 Ga (Schröder et al., 2016). This suggests that the Makganyene diamictite

Table 3

Samarium-Nd concentrations and $^{143}Nd/^{144}Nd$ isotopic data. Errors given are 2SE of individual analysis. T_{DM} – Neodymium model age. Depleted mantle model ages (T_{DM}) were calculated using a depleted mantle from Goldstein et al. (1984). Epsilon Nd values were calculated relative to a chondritic model mantle with the isotope compositions defined by Bouvier et al. (2008). $\varepsilon Nd_{(T)}$ are epsilon Nd values calculated at the maximum depositional age, which are from [1]Kositcin and Krapež (2004), [2]Mukasa et al. (2013), [3]Rasmussen et al. (2013), [4]Prave et al. (2016), [5]Isbell et al. (2008).

| Sample	Nd [ppm]	Sm [ppm]	$^{143}Nd/^{144}Nd$	$^{147}Sm/^{144}Nd$	T_{DM} [Ma]	$\varepsilon Nd_{(T)}$	Age of deposition [Ma]
Promise	11.26	2.136	0.510978 (5)	0.1147	3310	−1.0	2980 [1]
Mozaan	10.50	1.996	0.510997 (5)	0.1150	3290	−0.8	2980 [2]
Makganyene	16.11	3.003	0.511161 (5)	0.1127	2970	−2.6	2430 [3]
Timeball Hill	26.55	4.695	0.511118 (5)	0.1069	2870	−3.6	2260 [3]
Ghaub	14.74	2.905	0.512010 (5)	0.1191	1820	−5.8	640 [4]
Dwyka West	16.02	3.117	0.511548 (6)	0.1176	2520	−18.0	310 [5]
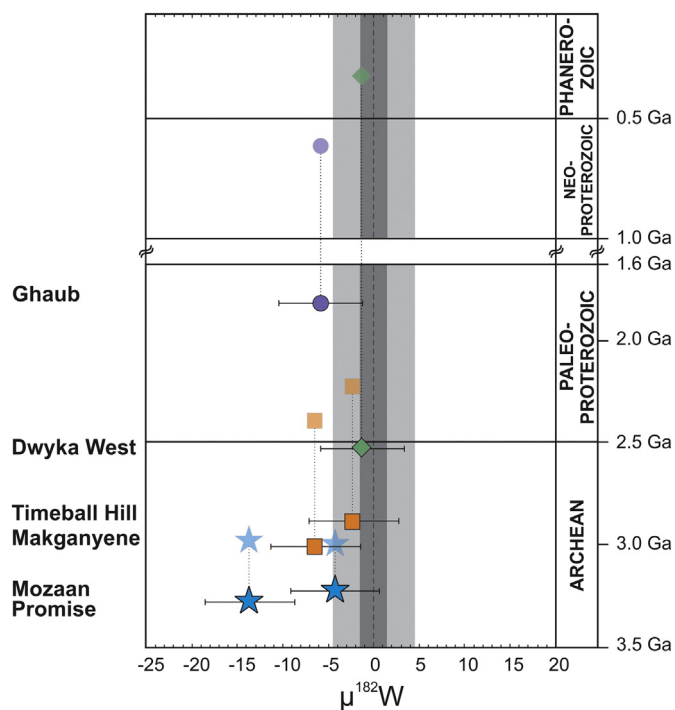
Fig. 5. Calculated Nd model ages (T_{DM}) of six southern African diamictite composites vs. $\mu^{182}W$. Y-axis represents ages from 3.5 Ga ago until today. Faded symbols represent the samples' glacial deposition ages. Darker symbols are the calculated T_{DM}. Associated sample symbols are connected by dotted lines.

Fig. 6. Average concentrations of Os + Ir + Ru in ppb (a) and Ni concentrations in ppm (b), of glacial diamictite composites vs. $\mu^{182}W$. The HSE data are from Chen et al. (2016) and the Ni data from Gaschnig et al. (2016).

tapped a Paleoarchean provenance that is largely absent from Timeball Hill.

The Neoproterozoic Ghaub diamictite, which was deposited between 0.64 and 0.65 Ga (Prave et al., 2016), yields a Nd T_{DM} model age of 1.8 Ga. No zircon data are available for this sample; however, the Paleoproterozoic T_{DM} model age suggests crustal components that are significantly older than the depositional age. The Ghaub diamictite is characterized by a $\mu^{182}W$ value of −5.9 ± 4.5, which is unresolved from the 2SE of the laboratory standard.

The two Paleoproterozoic diamictites, Duitschland and Bruce, and the Neoproterozoic diamictites, Pocatello and Gaskiers all have W isotopic compositions that are not resolved from the 2SE of the laboratory standard. Thus, by this time in Earth history, ^{182}W isotopic heterogeneity in this portion of the UCC (and by inference, the upper mantle from which it was derived) appears to have disappeared.

The Phanerozoic Dwyka West and Bolivia diamictites are both also characterized by normal W isotopic compositions. The largest discrepancy between deposition and T_{DM} ages of the diamictite suite is found for the Dwyka West diamictite composite. This formation was deposited ~0.3 Ga ago, yet it is also characterized by an Archean T_{DM} age of 2.5 Ga, indicative of a large contribution from Archean crustal
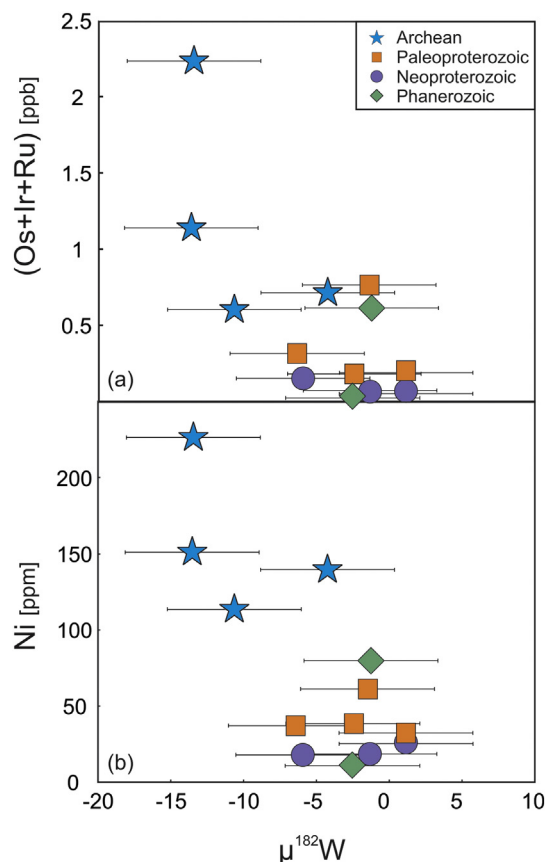
components. Further, the comparatively high HSE and transition metal concentrations are consistent with substantial input from ultramafic sources (Chen et al., 2016; Gaschnig et al., 2014). The ancient nature of the provenance is also reflected in zircon populations. Data from Cornell et al. (2011) from a Dwyka outcrop further to the northwest of this study's composite sampling locality shows age peaks of up to 3.1 Ga, consistent with several Mesoarchean crustal sources. The lack of ^{182}W anomalies in the Dwyka West composite sample either indicates that the negative $\mu^{182}W$ values present in the UCC sources for the older South African diamictites have disappeared by 3.1 Ga in this region, which, according to zircon data, are the oldest identified crustal components of the Dwyka West formation, or the normal ^{182}W signatures present in younger components dominated any components with anomalous isotopic compositions. A swamping of the signal could have occurred because potentially older ultramafic source components are generally characterized by much lower W concentrations than in more felsic rocks. Hence, although older, ultramafic components in the

Dwyka West sample may be reflected in the HSE and compatible transition element concentrations of this composite, these source components, potentially characterized by a negative μ^{182}W values, may have been significantly diluted by younger, felsic materials with normal W isotopic compositions and much higher W concentrations.

An alternative explanation for the normal ^{182}W signature of the Dwyka West diamictite, despite apparently comprising large amounts of ultramafic components, is that not all ultramafic rocks are characterized by anomalous ^{182}W compositions. For example, the Paleoarchean Komati komatiites, Barberton Greenstone Belt, South Africa, show no ^{182}W anomalies (Touboul et al., 2012). Thus, at least some Archean ultramafic rocks were derived from deep mantle sources lacking ^{182}W anomalies.

We conclude that differences in the glacier's provenance for individual diamictite formations may explain the differences in the measured μ^{182}W values in samples with similarly high ultramafic/felsic component ratios. Hence, elevated HSE in the diamictites, indicative of high contents of ultramafic components may not necessarily translate into anomalous ^{182}W signatures.

6. Conclusions

- Tungsten isotopic studies of glacial diamictites are characterized by negative μ^{182}W values in samples deposited in South Africa during the Mesoarchean. This observation, coupled with published data showing both positive and negative anomalies in various crustal rocks is consistent with the conclusion that the UCC at that time, and, by inference, the upper mantle from which it derived, was quite heterogeneous with respect to μ^{182}W.

- A correlation of μ^{182}W with the proportion of ultramafic (komatiitic) components in diamictite composites suggests that komatiites may have been a major source of the anomalous ^{182}W signatures observed in the South African Archean samples. If so, this likely reflects deeper mantle source reservoirs for komatiites, suggesting that the lower mantle may preserve ^{182}W signatures longer in Earth's history than the upper mantle.

- T$_{DM}$ model ages determined for six of the glacial diamictite composites are, in all cases, significantly older than the ages of glacial deposition. Mesoarchean model ages combined with published detrital zircon U-Pb ages for the Paleoproterozoic Makganyene Formation suggests significant amounts of early Archean crustal components that may be responsible for the small negative μ^{182}W signature observed in the Makganyene diamictite.

- The decrease and eventual disappearance of anomalous ^{182}W signatures in diamictite formations deposited during the Proterozoic and Phanerozoic indicates homogenization of W isotopes in the continental crust and upper mantle with time.

Supplementary data to this article can be found online at https://doi.org/10.1016/j.chemgeo.2018.07.036.

References

Archer, G.J., Mundl, A., Walker, R.J., Worsham, E.A., Bermingham, K.R., 2017. High-

precision analysis of ^{182}W/^{184}W and ^{183}W/^{184}W by negative thermal ionization mass spectrometry: per-integration oxide corrections using measured ^{18}O/^{16}O. Int. J. Mass Spectrom. 414, 80–86. https://doi.org/10.1016/j.ijms.2017.01.002.

Arevalo Jr., R., McDonough, W.F., 2008. Tungsten geochemistry and implications for understanding the Earth's interior. Earth Planet. Sci. Lett. 272, 656–665. https://doi.org/10.1016/j.epsl.2008.05.031.

Bouvier, A., Vervoort, J.D., Patchett, P.J., 2008. The Lu-Hf and Sm-Nd isotopic composition of CHUR: Constraints from unequilibrated chondrites and implications for the bulk composition of terrestrial planets. Earth Planet. Sci. Lett. 273, 48–57. https://doi.org/10.1016/j.epsl.2008.06.010.

Bowring, S., Myrow, P., Landing, E., Ramezani, J., Grotzinger, J., 2003. Geochronological Constraints on Terminal Neoproterozoic Events and the Rise of Metazoan. NASA Astrobiol. Inst, pp. 113–114 (Gen. Meet. Abst.).

Cawood, P.A., Kroner, A., Dhuime, B., 2013. The continental record and the generation of the continental crust. Geol. Soc. Am. Bull. 125, 14–32. https://doi.org/10.1130/B30722.1.

Chen, K., Walker, R.J., Rudnick, R.L., Gao, S., Gaschnig, R.M., Puchtel, I.S., Tang, M., Hu, Z.-C., 2016. Platinum-group element abundances and Re–Os isotopic systematics of the upper continental crust through time: evidence from glacial diamictites. Geochim. Cosmochim. Acta 191, 1–16. https://doi.org/10.1016/j.gca.2016.07.004.

Condie, K.C., 1993. Chemical composition and evolution of the upper continental crust: Contrasting results from surface samples and shales. Chem. Geol. 104, 1–37. https://doi.org/10.1016/0009-2541(93)90140-E.

Cornell, D.H., van Schijndel, V., Ingolfsson, O., Schersten, A., Karlsson, L., Wojtyla, J., Karlsson, K., 2011. Evidence from Dwyka tillite cobbles of Archean basement beneath the Kalahari sands of southern Africa. Lithos 152, 482–502. https://doi.org/10.1016/j.lithos.2011.03.006.

Dale, C.W., Kruijer, T.S., Burton, K.W., 2017. Highly siderophile element and ^{182}W evidence for a partial late veneer in the source of 3.8 Ga rocks from Isua, Greenland. Earth Planet. Sci. Lett. 458, 394–404. https://doi.org/10.1016/j.epsl.2016.11.001.

Dhuime, B., Hawkesworth, C.J., Cawood, P.A., Storey, C.D., 2012. A change in the geodynamics of continental growth 3 billion years ago. Science 335, 1334–1336. https://doi.org/10.1126/science.1216066.

Dhuime, B., Wuestfeld, A., Hawkesworth, J., 2015. Emergence of modern continental crust about 3 billion years ago. Nat. Geosci. 8, 552–555. https://doi.org/10.1038/ngeo2466.

Gao, S., Luo, T.-C., Zhang, B.-R., Zhang, H.-F., Han, Y.-W., Zhao, Z.-D., Hu, Y.-K., 1998. Chemical composition of the continental crust as revealed by studies in East China. Geochim. Cosmochim. Acta 62, 1959–1975. https://doi.org/10.1016/S0016-7037(98)00121-5.

Garçon, M., Carlson, R.W., Shirey, S.B., Arndt, N.T., Horan, M.F., Mock, T.D., 2017. Erosion of Archean continents: the Sm-Nd and Lu-Hf isotopic record of Barberton sedimentary rocks. Geochim. Cosmochim. Acta 206, 216–235.

Gaschnig, R.M., Rudnick, R.L., McDonough, W.F., Kaufman, A.J., Hu, Z., Gao, S., 2014. Onset of oxidative weathering of continents recorded in the geochemistry of ancient glacial diamictites. Earth Planet. Sci. Lett. 408, 87–99. https://doi.org/10.1016/j.epsl.2014.10.002.

Gaschnig, R.M., Rudnick, R.L., McDonough, W.F., Kaufman, A.J., Valley, J.W., Hu, Z., Gao, S., Beck, M.L., 2016. Compositional evolution of the upper continental crust through time, as constrained by ancient glacial diamictites. Geochim. Cosmochim. Acta 186, 316–343. https://doi.org/10.1016/j.gca.2016.03.020.

Goldstein, S.L., O'Nions, R.K., Hamilton, P.J., 1984. A Sm-Nd isotopic study of atmospheric dusts and particulates from major river systems. Earth Planet. Sci. Lett. 70, 221–236. https://doi.org/10.1016/0012-821X(84)90007-4.

Gumsley, A.P., Chamberlain, K.R., Bleeker, W., Soederlund, U., de Kock, M.O., Larsson, E.R., Bekker, A., 2017. Timing and tempo of the Great Oxidation Event. PNAS 114, 1811–1816. https://doi.org/10.1073/pnas.1608824114.

Hawkesworth, C.J., Cawood, P.A., Dhuime, B., 2013. Continental growth and the crustal record. Tectonophysics 609, 651–660. https://doi.org/10.1016/j.tecto.2013.08.013.

Herzberg, C., 1992. Depth and degree of melting komatiites. J. Geophys. Res. 97, 4521–4540. https://doi.org/10.1029/91JB03066.

Herzberg, C., Condie, K., Korenaga, J., 2010. Thermal history of the Earth and its petrological expression. Earth Planet. Sci. Lett. 292, 79–88. https://doi.org/10.1016/j.epsl.2010.01.022.

Isbell, J.L., Cole, D.I., Catuneanu, O., 2008. Carboniferous-Permian glaciation in the main Karoo Basin, South Africa: Stratigraphy, depositional controls, and glacial dynamics. Bull. Geol. Soc. Am. 441, 71–82. https://doi.org/10.1130/2008.2441(05).

Keeley, J.A., Link, P.K., Fanning, C.M., Schmitz, M.D., 2013. Pre- to synglacial rift-related volcanism in the Neoproterozoic (Cryogenian) Pocatello Formation, SE Idaho: New SHRIMP and CA-ID-TIMS constraints. Lithosphere 5, 128–150. https://doi.org/10.1130/L226.1.

Kleine, T., Mezger, K., Muenker, C., Palme, H., Bischoff, A., 2004. ^{182}Hf-^{182}W isotope systematics of chondrites, eucrites, and martian meteorites: Chronology of core formation and early mantle differentiation in Vesta and Mars. Geochim. Cosmochim. Acta 68, 2935–2946. https://doi.org/10.1016/j.gca.2004.01.009.

Kositcin, N., Krapež, B., 2004. Relationship between detrital zircon age spectra and the tectonic evolution of the Late Archaean Witwatersrand Basin, South Africa. Precambrian Res. 129, 141–168. https://doi.org/10.1016/j.precamres.2003.10.011.

Kruijer, T.S., Kleine, T., 2018. No 182W excess in the Ontong Java Plateau source. Chem. Geol. 485, 24–31. https://doi.org/10.1016/j.chemgeo.2018.03.024.

Langmuir, D., Herman, J.S., 1980. The mobility of thorium in natural waters at low temperatures. Geochim. Cosmochim. Acta 44, 1753–1766. https://doi.org/10.1016/0016-7037(80)90226-4.

Li, S., Gaschnig, R.M., Rudnick, R.L., 2016. Insights into chemical weathering of the upper continental crust from the geochemistry of ancient glacial diamictites. Geochim. Cosmochim. Acta 176, 96–117. https://doi.org/10.1016/j.gca.2015.12.012.

Liu, J., Touboul, M., Ishikawa, A., Walker, R.J., Pearson, D.G., 2016. Widespread tungsten isotope anomalies and W mobility in crustal and mantle rocks of the Eoarchean Saglek Block, northern Labrador, Canada: implications for early Earth processes and W recycling. Earth Planet. Sci. Lett. 448, 13–23. https://doi.org/10.1016/j.epsl.2016.05.001.

Moore, J.M., Polteau, S., Armstrong, R.A., Corfu, F., Tsikos, H., 2012. The age and correlation of the Postmasburg Group, southern Africa: Constraints from detrital zircon grains. J. Afr. Earth Sci. 64, 9–19. https://doi.org/10.1016/j.afrearsci.2011.11.001.

Mukasa, S.B., Wilson, A.H., Young, K.R., 2013. Geochronological constraints on the magmatic and tectonic development of the Pongola Supergroup (Central Region), South Africa. Precambrian Res. 224, 268–286. https://doi.org/10.1016/j.precamres.2012.09.015.

Mundl, A., Touboul, M., Jackson, M.G., Day, J.M.D., Kurz, M.D., Lekic, V., Helz, R.T., Walker, R.J., 2017. Tungsten-182 heterogeneity in modern ocean island basalts. Science 356, 66–69. https://doi.org/10.1126/science.aal4179.

Nan, X.-Y., Yu, H.-M., Rudnick, R.L., Gaschnig, R.M., Xu, J., Li, W.Y., Zhang, Q., Jin, Z.-D., Li, X.-H., Huang, F., 2018. Barium isotopic composition of the upper continental crust. Geochim. Cosmochim. Acta 233, 33–49. https://doi.org/10.1016/j.gca.2018.05.004.

Prave, A.R., Condon, D.J., Hoffmann, K.H., Tapster, S., Fallick, A.E., 2016. Duration and nature of the end-Cryogenian (Marinoan) glaciation. Geology 44, 631–634. https://doi.org/10.1130/G38089.1.

Puchtel, I.S., Bruegmann, G.E., Hofmann, A.W., 2001. [187]Os-enriched domain in an Archean mantle plume: evidence from 2.8 Ga komatiites of the Kostomuksha greenstone belt, NW Baltic Shield. Earth Planet. Sci. Lett. 186, 513–526. https://doi.org/10.1016/S0012.821X(01)00264-3.

Puchtel, I.S., Blichert-Toft, J., Touboul, M., Horan, M.F., Walker, R.J., 2016. The coupled [182]W-[142]Nd record of early terrestrial mantle differentiation. Geochem. Geophys. Geosyst. 17, 2168–2193. https://doi.org/10.1002/2016GC006324.

Puchtel, I.S., Blichert-Toft, J., Touboul, M., Walker, R.J., 2018. [182]W and HSE constraints from 2.7 Ga komatiites on the heterogeneous nature of the Archean mantle. Geochim. Cosmochim. Acta 228, 1–26. https://doi.org/10.1016/j.gca.2018.02.030.

Rasmussen, B., Bekker, A., Fletcher, I.R., 2013. Correlation of Paleoproterozoic glaciations based on U–Pb zircon ages for tuff beds in the Transvaal and Huronian Supergroups. Earth Planet. Sci. Lett. 382, 173–180. https://doi.org/10.1016/j.epsl.2013.08.037.

Reimink, J.R., Chacko, T., Carlson, R.W., Shirey, S.B., Liu, J., Stern, R.A., Bauer, A.M., Pearson, G., Heaman, L.M., 2018. Petrogenesis and tectonics of the Acasta Gneiss complex derived from integrated petrology and [142]Nd and [182]W extinct nuclide-geochemistry. Earth Planet. Sci. Lett. 494, 12–22. https://doi.org/10.1016/j.epsl.2018.04.047.

Rizo, H., Walker, R.J., Carlson, R.W., Horan, M.F., Mukhopadhyay, S., Manthos, V., Francis, D., Jackson, M.G., 2016a. Preservation of Earth-forming events in the tungsten isotopic composition of modern flood basalts. Science 352, 809–812. https://doi.org/10.1126/science.aad8563.

Rizo, H., Walker, R.J., Carlson, R.W., Touboul, M., Horan, M.F., Puchtel, I.S., Boyet, M., 2016b. Early Earth differentiation investigated through [142]Nd, [182]W, and highly siderophile element abundances in samples from Isua, Greenland. Geochim. Cosmochim. Acta 175, 319–336. https://doi.org/10.1016/j.gca.2015.12.007.

Rudnick, R.L., Gao, S., 2014. Composition of the continental crust. In: Holland, H.D., Turekian, K.K. (Eds.), The Crust, Treatise on Geochemistry. vol. 4. Elsevier-Pergamum, Oxford, pp. 1–45.

Schröder, S., Beukes, N.J., Armstrong, R., 2016. Detrital zircon constraints on the tecto-nostratigraphy of the Paleoproterozoic Pretoria Group, South Africa. Precambrian Res. 278, 362–393. https://doi.org/10.1016/j.precamres.2016.03.016.

Shaw, D.M., Dostal, J., Keays, R.R., 1976. Additional estimates of continental surface Precambrian shield composition in Canada. Geochim. Cosmochim. Acta 40, 73–83. https://doi.org/10.1016/0016-7037(76)90195-2.

Starck, D., del Papa, C., 2006. The northwestern Argentina Tarija Basin: Stratigraphy, depositional systems, and controlling factors in a glaciated basin. J. S. Am. Earth Sci. 22, 169–184. https://doi.org/10.1016/j.jsames.2006.09.013.

Tang, M., Chen, K., Rudnick, R.L., 2016. Archean upper crust transition from mafic to felsic marks the onset of plate tectonics. Science 351, 372–375. https://doi.org/10.1126/science.aad5513.

Taylor, S.R., McLennan, S.M., 1985. The Continental Crust: Its Composition and Evolution. Blackwell, Oxford, pp. 315–327. https://doi.org/10.1002/gj.3350210116.

Touboul, M., Walker, R.J., 2012. High precision tungsten isotope measurement by thermal ionization mass spectrometry. Int. J. Mass Spectrom. 309, 109–117. https://doi.org/10.1016/j.ijms.2011.08.033.

Touboul, M., Puchtel, I.S., Walker, R.J., 2012. [182]W evidence for long-term preservation of early mantle differentiation products. Science 335, 1065–1069. https://doi.org/10.1126/science.1216351.

Touboul, M., Liu, J., O'Neil, J., Puchtel, I.S., Walker, R.J., 2014. New insights into the Hadean mantle revealed by [182]W and highly siderophile element abundances of su-pracrustal rocks from the Nuvvuagittuq Greenstone Belt, Quebec, Canada. Chem. Geol. 383, 63–75. https://doi.org/10.1016/j.chemgeo.2014.05.030.

Vockenhuber, C., Oberli, F., Bichler, M., Ahmad, I., Quitte, G., Meier, M., Halliday, A.N., Lee, D.-C., Kutschera, W., Steier, P., Gehrke, R.J., Helmer, R.G., 2004. New half-life measurement of [182]Hf: improved chronometer for the early solar system. Phys. Rev. Lett. 93, 1–4. https://doi.org/10.1103/PhysRevLett.93.172501.

Willbold, M., Elliott, T., Moorbath, S., 2011. The tungsten isotopic composition of the Earth's mantle before the terminal bombardment. Nature 477, 195–198. https://doi.org/10.1038/nature10399.